Chemical Science

Accepted Manuscript

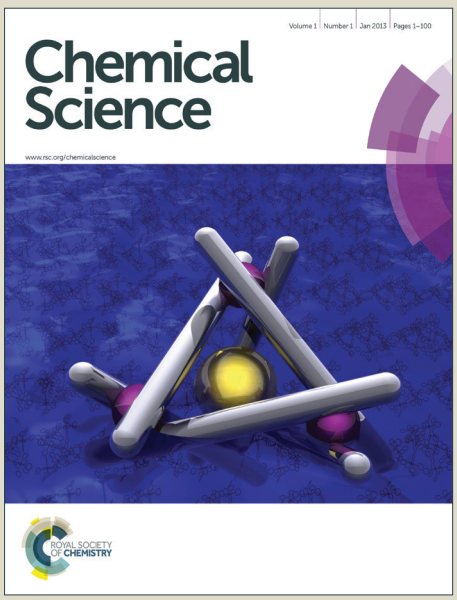

ROYAL SOCIETY OF CHEMISTRY

www.rsc.org/chemicalscience

Chemical Science

RSCPublishing

EDGE ARTICLE

Nanoconfining affinity materials for pH-mediated protein capture/release

Cite this: DOI: 10.1039/xoxxooooox

Qianjin Li, Xueying Tu, Jin Ye, Zijun Bie, Xiaodong Bi, and Zhen Liu*

Received ooth April 2014,
Accepted ooth April 2014

DOI: 10.1039/xoxxooooox

www.rsc.org/

Nanoconfinement effect may dramatically influence the physicochemical properties of substances. Porous materials have been widely used as separation media in liquid chromatography. However, the confinement effect of pores was usually considered as a detrimental factor. Here we report a novel type of functional materials, nanoconfining affinity materials (NCAMs), which rely on the nanoconfinement effect of porous materials with pore sizes comparable to the molecular sizes of proteins to provide dominate affinity. Two NCAMs that allow for pH-responsive capture/release of proteins were developed. The NCAMs could bind proteins with molecular mass larger than 18 kDa when the surrounding pH is ≥ 6.0 while the captured proteins could be reversibly released upon switching the environmental pH < 3.0. The dissociation constants for three test proteins ranged from 10^{-5} to 10^{-7} M. The NCAMs could well retain the conformation and activities of captured proteins. Promising applications of the NCAMs in enantiomer resolution, immobilized enzyme reactor and the depletion of serum proteins were demonstrated. The nanoconfining strategy opens up new avenues to the rational design of unique functional materials.

Introduction

Confinement effect of nanoscale spaces has attracted increasing attentions in multiple fields, from physics to chemistry to materials science. When a compound is confined in a limited space, its physicochemical properties, such as density,[1] rigidity,[2] reactivity,[3] catalytic activity,[4] and so on, may dramatically differ from those under non-confined conditions. Nanoconfinement effect often occurs in porous materials.[5] Porous materials have been widely used as separation media in liquid chromatography.[6] The size exclusion effect of nanopores has been well explored. Size exclusion chromatography (SEC) has been an important tool for the separation and molecular weight measurement of macromolecules,[7] while restricted access materials (RAMs) have been widely used for the selective extraction of small molecules from macromolecule-containing complex samples such as blood.[8] Besides, the size exclusion effect of nanopores has been utilized as a key factor for the design of biomimetic affinity materials.[9] However, the confinement effect of pores on the retention behaviors of analytes in chromatographic separations has never been well investigated. Particularly in affinity chromatography, conventional affinity media predominately relied on the properties of affinity ligands,[10] while the confinement effect of pores was usually considered as a detrimental factor so that the pore sizes were usually required to be at least 5-10 times larger than the sizes of the proteins to be separated.[11]

However, favorable effects of nanoconfinement in separation science have been continuously unveiled recently.[12,13] A finding by us[12] on molecularly imprinted polymers (MIPs), which are synthetic receptors mimicking the molecular recognition properties of antibodies and enzymes,[14] revealed that, due to the presence of nanoscale imprinted cavities, boronic acid-based MIPs can provide unexpected highly favorable affinity properties as compared with regular boronate affinity materials. Particularly, the binding strength toward template proteins was enhanced by 5 order of magnitude as compared with the binding in free solution.[15] We further observed that, confinement effect of imprinted cavities predominantly contributed to the binding strength of MIPs toward target.[13] More recently, we uncovered that molecular interactions confined within mesoporous silica were significantly enhanced as compared with those under non-confined conditions.[16] All these findings imply that nanoconfinement can be a new core element for the rational design of advanced functional materials.

Boronic acid-functionalized materials have found important applications in various fields such as separation,[17] sensing,[18] and drug delivery,[19] due to their unique pH-responsive reversible capture/release capability (high pH on/low pH off) toward *cis*-diol containing compounds especially glycoproteins. However, boronic acid-functionalized materials are not applicable to nonglycoproteins. Therefore, novel functional materials with pH-responsive capture/release ability toward both of nonglycoproteins and glycoproteins are of great importance.

Here we present a novel type of functional materials, nanoconfining affinity materials (NCAMs). NCAMs rely on a nanoconfining strategy: base porous materials with pore sizes comparable to the molecular sizes of the most frequently encountered proteins (~3-30 nm) can provide dominate affinity toward the proteins due to nanoconfinement effect. After being functionalized with appropriate ligands, the prepared NCAMs can provide designed affinity properties. Two base materials, polymer monoliths and microspheres, were used as base materials. Modified with *N*-(β-hydroxy propyl)ethylene diamine (HPEDA), NCAMs with boronate affinity-like pH-controlled binding properties toward proteins were developed. The NCAMs could bind proteins with

molecular mass larger than 18 kDa when the surrounding pH is equal to or higher than 6.0 while the captured proteins could be reversibly released upon switching the environmental pH less than 3.0 (Scheme 1). The dissociation constants for three test proteins ranged from 10^{-5} to 10^{-7} M. NCAMs could well retain the conformation and activities of captured proteins. Promising applications of the NCAMs in protein separation, enantiomer resolution and immobilized enzyme reactor were demonstrated.

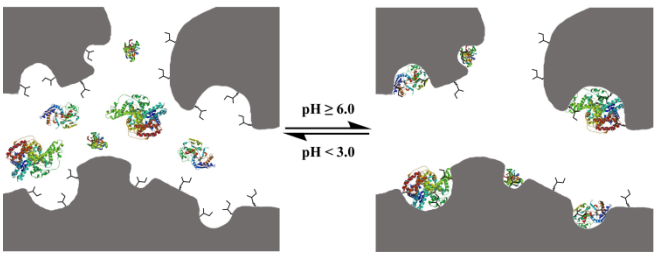

Scheme 1 Schematic illustration of pH-mediated protein capture and release by nanoconfining affinity materials.

Results and discussion

A base material and a ligand with appropriate nature are essential aspects to obtain pH-responsive binding properties. Methylene bisacrylamide (MBAA) was selected as a major polymerizing reagent to synthesize base materials for two reasons. First, it possesses good hydrophilicity, and thus unwanted interactions can be avoided. Second, it can provide pH-dependent interactions with amino acids. Its amide groups can function as both hydrogen bond donor and acceptor at a nearly neutral and alkaline pH (pH 6-10) and thus MBAA can interact with amino acids through hydrogen bonding. When the surrounding pH is switched to acidic (pH < 3.0), the amide groups and nearly all amino acids are positively charged, and thus the hydrogen bonding is offset by electrostatic repulsion. HPEDA was selected as the ligand. For one reason, similar to MBAA, HPEDA can function as both hydrogen bond donor and acceptor, but HPEDA can modulate a pH-switchable binding more efficiently due to its secondary amine, which has higher proton affinity as compared with primary amines. For the other reason, HPEDA groups can be easily obtained through ring-opening reaction. To provide an anchor for HPEDA attachment, glycidyl methacrylate (GMA) was used as a monomer to prepare base polymer monolith. The expected pH-dependent binding properties of MBAA and HPEDA toward amino acids were experimentally verified (Table S1). HPEDA exhibited limited affinity toward amino acids (dissociation constant K_d, 1-5 M) (Table S2). Due to multiple binding, however, HPEDA exhibited much higher affinity toward proteins in free solution (K_d, ~10^{-2} M) (Table S3).

We first synthesized a poly(MBAA) monolith with a certain population of nanopores (5-100 nm)[20] as a starting no-ligand NCAM (NL-NCAM) (Fig. 1a and 1b). The NL-NCAM captured bovine serum albumin (BSA) tightly but captured transferrin (Trans) and β-casein (β-Cas) loosely (Fig. 2a and 2b). The monolith exhibited high binding strength toward the three proteins (K_d, 10^{-5}-10^{-6} M) (Table 1). We prepared an HPEDA-immobilized organic-silica hybrid monolith without nanopore within 5-100 nm (HPEDA-NNCM) (Fig. 1c and 1d). Because of the absence of confining nanopores, the HPEDA-NNCM did not capture the test proteins at all (Fig. 2c and 2d). We further prepared an HPEDA-immobilized poly(MBAA-co-GMA) monolith with more desired nanopore distribution (nanopores of 5-50 nm with higher population) (Fig. 1e and 1f). The HPEDA-modified NCAM captured all the test proteins tightly at neutral pH while the captured proteins were eluted into sharp peaks by an acidic

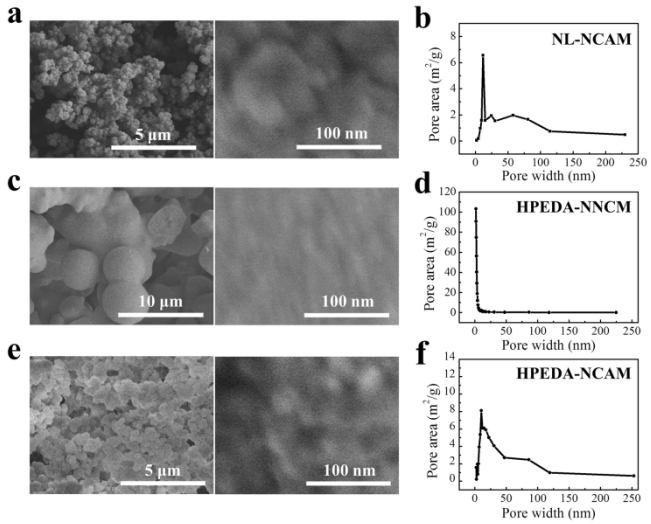

Fig. 1 Scanning electron microscopic images (a, c, e) and pore size distribution (b, d, f) of NL-NCAM (a, b); HPEDA-NNCM (c, d) and HPEDA-NCAM (e, f).

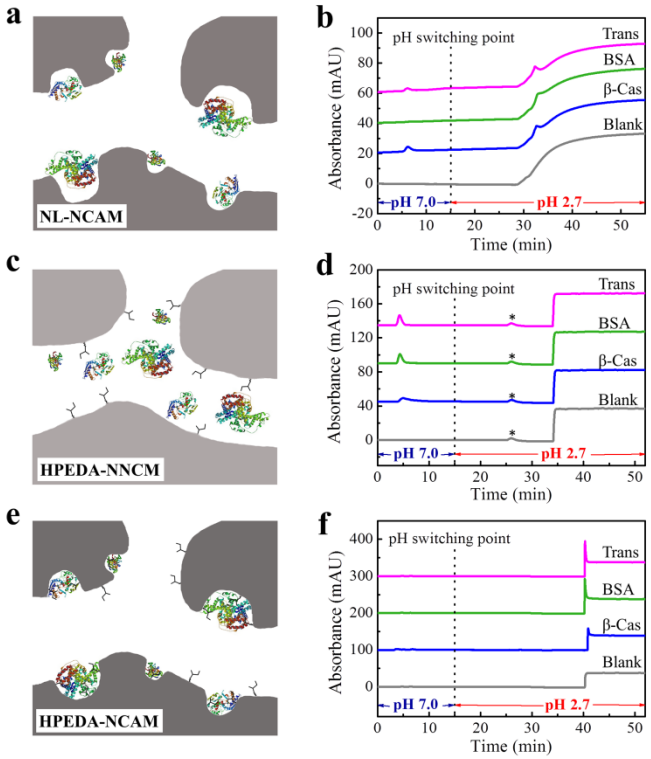

Fig. 2 (a) Illustration showing NL-NCAM exhibits a certain affinity toward the test proteins with different molecular sizes; (b) Chromatograms of the test proteins on NL-NCAM; (c) Illustration showing HPEDA-NNCM exhibits no affinity toward the test proteins; (d) Chromatograms of the test proteins on HPEDA-NNCM; (e) Illustration showing HPEDA-NCAM exhibits improved affinity toward the test proteins; (f) Chromatograms of the test proteins on HPEDA-NCAM. *, system peak due to pH switching.

pH (Fig. 2e and 2f). The dissociation constants of the NCAM toward the test proteins were 10^{-6}-10^{-7} M (Table 1), which was improved apparently as compared with the starting poly(MBAA) monolith. Fig. S5 shows the affinity retention of 18 proteins on the HPEDA-NCAM. Cytochrome C, RNase A and myoglobin were not captured by the HPEDA-NCAM. Lysozyme was partially captured. While other proteins (with molecular weight > 18 kDa) were all captured by the HPEDA-NCAM. The zero-retention of cytochrome C, RNase A and myoglobin is assigned to their smaller molecular sizes as compared with the nanopores of the material (Table S5). The partial retention of lysozyme on the NCAM is attributed to electrostatic attraction (Fig. S6). While the retention behaviours of other proteins are attributed to the confinement effect of the nanopores that are comparable to the size of these proteins. The binding behaviours of a variety of proteins on the NCAM within the pH range of 6.0-10.0 obeyed the same pattern (Table S6).

Table 1 Dissociation constants of proteins with different materials

Material	Protein	K_d (M)	r [a]	Q_{max} (mg/g)
NL-NCAM	Trans	$(1.7\pm0.3)\times10^{-5}$	0.935	2.0
NL-NCAM	BSA	$(2.2\pm0.4)\times10^{-6}$	0.954	4.1
NL-NCAM	β-Cas	$(1.1\pm0.1)\times10^{-5}$	0.982	10.5
HPEDA-NCAM	Trans	$(7.2\pm0.7)\times10^{-6}$	0.972	3.8
HPEDA-NCAM	BSA	$(3.4\pm0.7)\times10^{-7}$	0.950	24.1
HPEDA-NCAM	β-Cas	$(2.5\pm0.4)\times10^{-6}$	0.930	26.9
HPEDA-NCAMB	Trans	$(2.7\pm0.3)\times10^{-5}$	0.982	10.4
HPEDA-NCAMB	BSA	$(1.6\pm0.3)\times10^{-6}$	0.923	68.3
HPEDA-NCAMB	β-Cas	$(2.3\pm0.2)\times10^{-5}$	0.977	425.8

[a] "*r*" means correlation coefficient.

The retention behaviors of peptides from tryptic digests of transferrin, BSA and ovalbumin on the HPEDA-NCAM column were examined. As shown in Fig. S7, except for a few peptides from transferrin digest that were adsorbed through electrostatic interaction, the peptides almost had no retention on the column, which conversely confirmed that the retention of the proteins on the HPEDA-NCAM column was due to nanoconfinement effect.

To evaluate the generality of the nanoconfining strategy, Profinity™ epoxide resin, a commercial macroporous microsphere, was employed as another base material. The microsphere exhibited nanopore population within 5-100 nm (Fig. S8). After modified with HPEDA, the obtained NCAM exhibited apparent binding capability toward proteins with molecular weight more than 18 kDa (Fig. S9). Its dissociation constants toward BSA, Trans and β-Cas ranged from 10^{-5} to 10^{-6} M (Table 1).

To evaluate the binding capability toward more proteins, human serum proteins were extracted by the HPEDA-modified nanoconfining monolith and the extracted proteins were analyzed by matrix-assisted laser desorption/ionization time-of-flight mass spectrometry (MALDI-TOF MS). Fig. 3 compares the MS spectra for the samples with and without extraction. When the serum sample was directly analyzed, totally 22 peaks were observed (Fig. 3a). When the serum sample was treated by the HPEDA-NCAM prior to MS analysis, totally 20 peaks were observed (Fig. 3b). The identities of the detected proteins are listed in Table S7. A protein that the HPEDA-NCAM failed to capture was glutathionylated transthyretin (14 kDa), which is attributed to its smaller molecular size. The intensities for individual peaks for the samples with and without extraction are different, which is due to the different relative abundances of the nanopores and the human serum proteins.

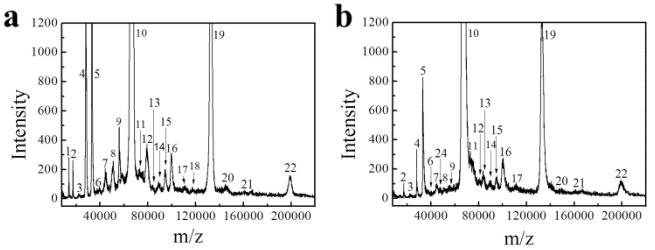

Fig. 3 (a) MALDI-TOF mass spectrum of human serum proteins; (b) MALDI-TOF mass spectrum of proteins captured by HPEDA-NCAM from human serum.

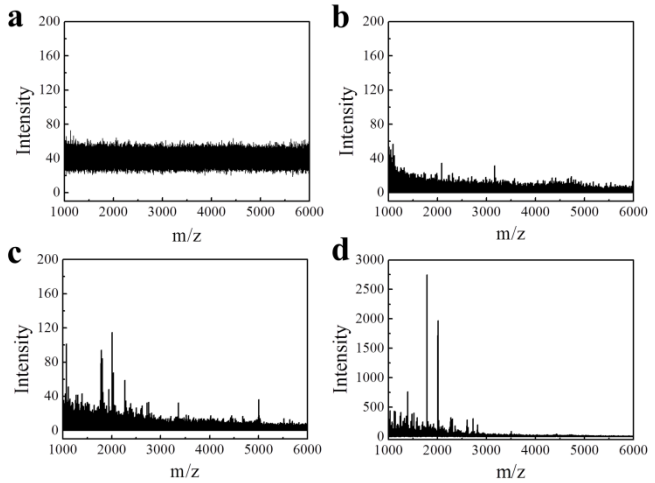

Fig. 4 (a) MALDI-TOF MS spectra of 10-fold diluted human serum; (b) MS spectra of captured components from 10-fold diluted human serum by C18 Zip-Tip; (c) MS spectra of flow through fraction of 10-fold diluted human serum after passing through HPEDA-NCAM column; (d) MS spectra of captured components from the flow through fraction (c) by C18 Zip-Tip.

The NCAMs could well retain the conformation and activities of captured proteins. Proteins are important chiral selectors for enantiomer resolution, and their chiral resolving capability highly depends on their conformation. Human serum albumin (HSA) possesses a L-tryptophan binding site at native status.[21] Fig. S10 shows that racemic tryptophan was separated into D and L forms by an HSA-bound NCAM column. Besides, enzymatic activities highly depend on the conformation of the proteins. As shown in Fig. S11 and Table S8, a trypsin-bound NCAM column could completely digest HRP into peptides within 2 h, with which totally 21 unique

peptides were identified. Such an enzymatic activity was comparable to the level reported in literature.[22] Since the desired properties of captured proteins still remained, NCAMs provide general supporting materials for easy fabrication of chiral separation columns and immobilized enzyme reactors.

Biomarkers studies revealed that the low-molecular-weight region of a proteome from body fluids is a rich source of information for the discovery of disease biomarkers.[23] However, the presence of high-abundance proteins severely suppresses the MS signals of low-abundance low-molecular-weight proteins. As such, the depletion of high-abundance proteins is a key step for the proteomic analysis of low-molecular weight proteome.[24] As shown in Fig. 3, high-abundance proteins in serum are all high-molecular-weight proteins, therefore, the HPEDA-NCAM monolith can be a useful material for the depletion of high-abundance serum proteins. As shown in Fig. 4a, when a serum sample was directly analyzed by MALDI-TOF MS, no peaks but strong noises were observed within the m/z range of 1,000-6,000. After the sample was treated with a C18 Zip-Tip, which is a widely used desalting tool in proteomic analysis, only a few peaks were observed (Fig. 4b), though the noise level was reduced. After the depletion of the high-abundance serum proteins by the HPEDA-NCAM, 13 peptides were detected from the flow through fraction (Fig. 4c). After the flow through fraction was further desalted by C18 Zip-Tip, totally 67 peptides were detected (Fig. 4d). All of the observed and identified peptides were listed in Table S9. Clearly, the HPEDA-NCAM exhibited a great potential for the depletion of high-abundance serum proteins and improvement of MS detection capability toward serum peptides. As compared with commercial multi-antibody immuneaffinity columns,[25] the NCAM column possesses several significant advantages, including easier to prepare, more stable and much lower cost.

Conclusions

In this study, we have proposed a nanoconfining strategy for the development of new affinity materials. Two NCAMs that allow for pH-mediated protein capture/release have been developed. The boronate affinity-like pH-controlled binding properties allowed for easy separation of proteins from other species, providing an complementary tool to boronate affinity materials, which are only applicable to glycoproteins. In particular, the NCAMs exhibited a great promise for the depletion of high-abundance serum proteins for proteomic analysis. Since the conformation and activities of captured proteins could be well retained, the NCAMs provided a general supporting material for facile fabrication of protein-based chiral separation columns and immobilized enzymatic reactors. Although the current NCAMs could not provide target specificity, which is available via molecular imprinting, a significant advantage of NCAMs over MIPs is that no template molecules are needed. If base materials with narrowly dispersed nanopores are available in future, size-specific NCAMs can be possible. This strategy opens up new avenues for the rational design of unique functional materials.

Acknowledgements

We gratefully acknowledge the financial support from the Ministry of Science and Technology of China (Grant No. 2013CB911202), the National Natural Science Foundation of China (Grant Nos. 21275073 and 21121091), the Natural Science Foundation of Jiangsu Province, China (Grant No. KB2011054), and the Program B for Outstanding PhD Candidate of Nanjing University (2013-2014). We greatly appreciate Ms. Youyi Peng's valuable suggestions on ligand-protein interactions.

Notes and references

State Key Laboratory of Analytical Chemistry for Life Science School of Chemistry and Chemical Engineering Nanjing University 22 Hankou Road, Nanjing 210093 (China) Fax: (+86) 25-8368-5639

E-mail: zhenliu@nju.edu.cn

† Electronic Supplementary Information (ESI) available: materials and methods, supporting tables and figures, See DOI: 10.1039/b000000x/

1. M. Heuberger, M. Zach and N. D. Spencer, *Science*, 2001, **292**, 905-908.
2. J. Klein and E. Kumacheva, *Science*, 1995, **269**, 816-819.
3. R. Gounder and E. Iglesia, *Angew. Chem. Int. Ed.*, 2010, **49**, 808-811.
4. Q. Fu, W. X. Li, Y. Yao, H. Liu, H. Y. Su, D. Ma, X. K. Gu, L. Chen, Z. Wang, H. Zhang, B. Wang and X. Bao, *Science*, 2010, **328**, 1141-1144.
5. (a) M.K. Kidder, P.F. Britt, Z.T. Zhang, S.Dai, E.W. Hagaman, A.L.Chaffee, A.C. Buchanan, *J. Am. Chem. Soc.* 2005, **127**, 6353-6360; (b) F.S. Schultz and M.A. Anderson, *J. Am. Chem. Soc.* 1999, **121**, 4933-4940; (c) C.H. Turner, J.K. Brennan, J.K. Johnson and K.E. Gubbins, *J. Chem. Phys.* 2002, **216**, 2138-2148.
6. (a) N. T. Miller, B. Feibush and B. L. Karger, *J. Chromatogr.*, 1984, **316**, 519-536; (b) K. Nakanishi and N. Tanaka, Acc. Chem. Res. 2007, 40, 863-873; (c) Y. Wang, F. Ai, S.C. Ng and T.T.Y. Tan, *J. Chromatogr. A*, 2012, **1128**, 99-119.
7. (a) J. Porath and P. Flodin, *Nature*, 1959, **183**, 1657-1659; (b) J. R. Whitaker, *Anal. Chem.*, 1963, **35**, 1950-1953; (c) D. Berek, *J. Sep. Sci.*, 2010, **33**, 315-335.
8. (a) P. Sadilek, D. Satinsky and P. Solich, *Trends Anal. Chem.*, 2007, **26**, 375-384; (b) S. H. Yang, H. Fan, R. J. Classon and K. A. Schug, *J. Sep. Sci.*, 2013, **36**, 2922-2938.
9. Y. C. Liu, Y. Lu and Z. Liu, *Chem. Sci.*, 2012, **3**, 1467-1471.
10. (a) J. C. Janson and J. A. Jonsson, in *Protein purification: principles, high resolution methods, and applications*, ed. J. C. Janson, John Wiley & Sons, Inc., Hoboken, 3 edn., 2011, vol. Vol. 2, pp. 23-278; (b) P. Bailon and D. V. Weber, *Nature*, 1988, **335**, 839-840.
11. (a) J. Nawrocki, *Chromatographia*, 1991, **31**, 177-192; (b) B. M. Wagner, S. A. Schuster, B. E. Boyes and J. J. Kirkland, *J. Chromatogr. A* 2012, **1264**, 22-30.
12. L. Li, Y. Lu, Z. J. Bie, H. Y. Chen and Z. Liu, *Angew. Chem. Int. Ed.* , 2013, **52**, 7451-7454.
13. S. S. Wang, J. Ye, Z. J. Bie and Z. Liu, *Chem. Sci.*, 2014, **5**, 1135-1140.
14. (a) G. Wulff and A. Sarhan, *Angew. Chem. Int. Ed.*, 1972, **11**, 341-345; (b) G. Vlatakis, L. I. Andersson, R. Muller and K. Mosbach, *Nature*, 1993, **361**, 645-647; (c) Y. Hoshino, T. Kodama, Y. Okahata and K. J. Shea, *J. Am. Chem. Soc.*, 2008, **130**, 15242-15243; (d) Y. Hoshino, H. Koide, T. Urakami, H. Kanazawa, T. Kodama, N. Oku and K. J. Shea, *J. Am. Chem. Soc.*, 2010, **132**, 6644-6645.
15. C. C. Lü, H. Y. Li, H. Y. Wang and Z. Liu, *Anal. Chem.*, 2013, **85**, 2361-2369.

16. Y. Chen, S. S. Wang, J. Ye, Z. Liu and X. C. Wu, *Nanoscale*, 2014, in press (DOI: 10.1039/C4NR01440E).
17. (a) L. B. Ren, Z. Liu, Y. C. Liu, P. Dou and H. Y. Chen, *Angew. Chem. Int. Ed.*, 2009, **48**, 6704-6707; (b) L. Liang and Z. Liu, *Chem. Commun.*, 2011, **47**, 2255-2257; (c) H. Y. Li and Z. Liu, *Trends Anal. Chem.*, 2012, **37**, 148-161; (d) H. Y. Wang, Z. J. Bie, C. C. Lü and Z. Liu, *Chem. Sci.*, 2013, **4**, 4298-4303; (e) R. Nishiyabu, Y. Kubo, T. D. James and J. S. Fossey, *Chem. Commun.* , 2011, **47**, 1106-1123..
18. T. D. James, K. Sandanayake and S. Shinkai, *Angew. Chem. Int. Ed.*, 1996, **35**, 1910-1922.
19. S. Mura, J. Nicolas and P. Couvreur, *Nat. Mater.*, 2013, **12**, 991-1003.
20. The pore sizes were analyzed at dry status by Barrett-Joyner-Halenda (BJH) method, but the materials were used at wet status in this study. Wet status usually results in swelling of polymer materials. Therefore, the actual pore sizes of the materials under use should be smaller than the BJH pore sizes.
21. J. B. Swaney and I. M. Klotz, *Biochemistry*, 1970, **9**, 2570-2574.
22. J. Liu, F. Wang, H. Lin, J. Zhu, Y. Bian, K. Cheng and H. Zou, *Anal. Chem.*, 2013, **85**, 2847-2852.
23. E. F. Petricoin, C. Belluco, R. P. Araujo and L. A. Liotta, *Nat. Rev. Cancer,* 2006, **6**, 961-967.
24. (a) R. S. Tirumalai, K. C. Chan, D. A. Prieto, H. J. Issaq, T. P. Conrads and T. D. Veenstra, *Mol. Cell. Proteomics*, 2003, **2**, 1096-1103; (b) W. J. Qian, J. M. Jacobs, T. Liu, D. G. Camp and R. D. Smith, *Mol. Cell. Proteomics*, 2006, **5**, 1727-1744.
25. (a) W. J. Qian, D. T. Kaleta, B. O. Petritis, H. L. Jiang, T. Liu, X. Zhang, H. M. Mottaz, S. M. Varnum, D. G. Camp, L. Huang, X. M. Fang, W. W. Zhang and R. D. Smith, *Mol. Cell. Proteomics*, 2008, **7**, 1963-1973; (b) T. J. Shi, T. L. Fillmore, X. F. Sun, R. Zhao, A. A. Schepmoes, M. Hossain, F. Xie, S. Wu, J. S. Kim, N. Jones, R. J. Moore, L. Pasa-Tolic, J. Kagan, K. D. Rodland, T. Liu, K. Q. Tang, D. G. Camp, R. D. Smith and W. J. Qian, *PNAS,* 2012, **109**, 15395-15400.